European Polymer Journal 69 (2015) 472–482

Contents lists available at ScienceDirect

European Polymer Journal

journal homepage: www.elsevier.com/locate/europolj

Swelling behavior of thermosensitive nanocomposite hydrogels composed of oligo(ethylene glycol) methacrylates and clay

Mengge Xia [a,1], Weijie Wu [a,1], Fengwei Liu [a,1], Patrick Theato [b], Meifang Zhu [a,*]

[a] State Key Laboratory for Modification of Chemical Fibers and Polymer Materials, College of Materials Science and Engineering, Donghua University, 2999 North Renmin Road, Shanghai 201620, People's Republic of China
[b] Institute for Technical and Macromolecular Chemistry, University of Hamburg, Bundesstr. 45, D-20146 Hamburg, Germany

ARTICLE INFO

Article history:
Received 25 December 2014
Received in revised form 26 March 2015
Accepted 30 March 2015
Available online 17 April 2015

Keywords:
Nanocomposite hydrogel
Thermosensitivity
Oligo(ethylene glycol) methacrylate
2-(2-Methoxyethoxy) ethyl methacrylate
Volume phase transition temperature (VPTT)
Swelling/deswelling kinetics

ABSTRACT

Novel thermosensitive nanocomposite (NC) hydrogels have been synthesized by copolymerization of 2-(2-methoxyethoxy) ethyl methacrylate (MEO_2MA), oligo(ethylene glycol) methacrylate (OEGMA), and using inorganic clay as cross-linker via *in-situ* free radical polymerization. The structure and morphology of clay/P(MEO_2MA-*co*-OEGMA) NC hydrogels were characterized by Fourier transform infrared spectroscopy (FTIR), X-ray diffraction (XRD), and scanning electron microscopy (SEM), and the results indicated that the inorganic clay was uniformly dispersed in the NC hydrogels and obviously affected the network structure. Furthermore, physical properties such as equilibrium swelling/deswelling ratio, water retention, reversible thermosensitivity, and temperature dependence behaviors of NC hydrogels with different chemical compositions (molar ratio of comonomer, clay, and mass fraction of polymer) were investigated carefully. Moreover, the deswelling kinetics at specific temperature was studied, and the deswelling rates were well described with a first-order kinetics equation. The results indicated that the obtained NC hydrogels showed a controllable equilibrium swelling/deswelling behavior and possessed remarkable thermosensitivity. In addition, when the molar ratio of MEO_2MA and OEGMA was 80 mol%: 20 mol%, the equilibrium swelling ratio of NC hydrogels with 5 wt% clay reached 1640%, which is four times higher than that of *N,N′*-methylenebisacrylamide cross-linked hydrogels (410%). Consequently, this novel clay/P(MEO_2MA-*co*-OEGMA) NC hydrogel with interesting thermosensitive properties would be promising for potential applications, such as stimuli-responsive valve, drug delivery system, artificial muscle, and biosensor.

1. Introduction

Hydrogels are three-dimensional cross-linked hydrophilic polymer networks, which can absorb and retain large quantities of water [1,2]. Stimuli-responsive hydrogels can undergo significant physical or chemical changes in response to variations of external conditions, including temperature, pH, light, ionic strength, electric field, etc. [3–6]. These smart hydrogels have been widely used in many applications, such as drug delivery systems, scaffolds for tissue engineering, artificial muscles, stimuli-responsive optics and biosensors [7–10]. Typically, the most extensively studied smart hydrogels based on poly(*N*-isopropylacrylamide) (PNIPAM) are commonly used in biomedical areas, because its volume phase transition temperature (VPTT) around 32 °C is close to human physiological temperature [11–14]. With the advent of organic/inorganic nanocomposite materials, PNIPAM based

* Corresponding author. Tel.: +86 21 67792849; fax: +86 21 67792855.
E-mail address: zhumf@dhu.edu.cn (M. Zhu).
[1] Tel.: +86 21 67792849; fax: +86 21 67792855.

http://dx.doi.org/10.1016/j.eurpolymj.2015.03.072
0014-3057/

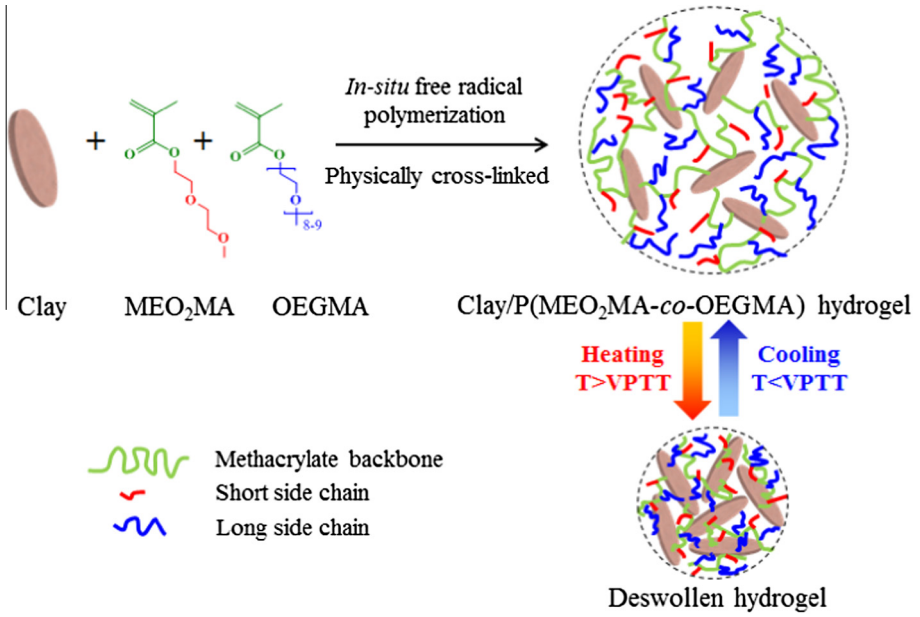

Scheme 1. Preparation of physically cross-linked clay/P(MEO_2MA-*co*-OEGMA) NC hydrogels.

nanocomposite (NC) hydrogels were also explored by using inorganic clay as physical cross-linkers instead of conventional organic cross-linkers. These NC hydrogels with inherent unique polymer/clay network structure exhibited excellent mechanical properties, controllable swelling/deswelling behavior, and reversible stimuli-responsiveness [15–19]. However, the application of these PNIPAM based NC hydrogels is limited because the employed monomer of *N*-substituted alkyl acrylamide is biology toxic, and its phase transition region is limited in a narrow range, both of which restrict their application in biomedical materials, drug release system and temperature responsive switches [20–23].

Recently, oligo(ethylene glycol) methacrylate (OEGMA) based polymers have gained increasing attention because of their biocompatibility and adjustable VPTT [24–26]. Lutz et al. first reported the thermosensitive copolymers by copolymerization of 2-(2-methoxyethoxy) ethyl methacrylate (MEO_2MA) and OEGMA units, showing obvious advantages such as non-toxicity, narrow hysteresis, and precisely tunable VPTT between 20 and 80 °C, which could be adjusted by the length of the side chains and the copolymer composition [27–29]. Subsequently, a large number of polymer micelles, polymer brushes, colloid, as well as a few of smart hydrogels based on MEO_2MA and OEGMA have been studied in detail [30–33]. Hu et al. synthesized thermosensitive P(MEO_2MA-*co*-OEGMA) microgels, which were cross-linked by ethylene glycol dimethacrylate and exhibited a controllable VPTT depending on the monomeric molar ratio [34,35]. Paris et al. prepared thermosensitive and thermo-/pH-sensitive hydrogels based on P(MEO_2MA-*co*-OEGMA) with tetraethylene glycol dimethacrylate as an organic cross-linker [36,37]. The swelling/deswelling properties and phase transition behaviors of the aforementioned chemically cross-linked hydrogels were reversible and can be precisely adjusted by the parameters such as monomeric composition, ionic strength, ethylene glycol side chain length, and environmental temperature.

To the best of our knowledge, these covalently cross-linked hydrogels based on P(MEO_2MA-*co*-OEGMA) featured low swelling ratios, insensitive phase transitions, and poor mechanical strength [38–40]. In this paper, we utilized inorganic clay as a physical cross-linker and prepared a series of thermosensitive clay/P(MEO_2MA-*co*-OEGMA) NC hydrogels by *in-situ* free radical polymerization of MEO_2MA and OEGMA in the presence of clay. The synthetic process and structural change near VPTT of clay/P(MEO_2MA-*co*-OEGMA) NC hydrogels are illustrated in Scheme 1. The chemical structure and morphology of the NC hydrogels were characterized by Fourier transform infrared (FTIR) spectroscopy, X-ray diffraction (XRD), and scanning electron microscopy (SEM). The effects of compositions (molar ratio of OEGMA, mass fractions of clay and polymer) on swelling/deswelling behavior, water retention, and reversible response of clay/P(MEO_2MA-*co*-OEGMA) NC hydrogels were carefully investigated.

2. Experimental

2.1. Materials

The monomers, 2-(2-methoxyethoxy) ethyl methacrylate (MEO_2MA, M_n = 188 g/mol) and oligo (ethylene glycol) methyl ether methacrylate (OEGMA, M_n = 475 g/mol), were purchased from Sigma–Aldrich and passed through silica gel column prior to use. The physical cross-linker clay (Laponite XLS, 92.32 wt% $[Mg_{5.34}Li_{0.66}Si_8O_{20}(OH)_4]Na_{0.66}$ and 7.68 wt% $Na_4P_2O_7$) with an average diameter of

approximately 30 nm and a thickness of 1 nm, was provided by Rockwood Ltd. UK. The chemical cross-linker *N,N′*-methylenebisacrylamide (NMBA), initiator potassium persulfate (KPS) and *N,N,N′,N′*-tetramethyl ethylene diamine (TEMED) were purchased from Sinopharm Chemical Reagent Co. Ltd. China. All the chemical reagents, except for the monomers, were used as received. The water used for all experiments was tapped from a Heal Force Bio-Meditech water purification system with a water resistivity of 18.2 MΩ cm.

2.2. Preparation of clay/P(MEO$_2$MA-co-OEGMA) hydrogels

The *in-situ* free radical polymerization of clay/P(MEO$_2$MA-*co*-OEGMA) NC hydrogels was carried out in aqueous solution consisting of monomers (MEO$_2$MA, OEGMA), cross-linker (inorganic clay), water, initiator (KPS), and accelerator (TEMED). All compositions of various hydrogels are listed in Table S1, and the synthesis procedure was as follows: A certain amount of inorganic clay, MEO$_2$MA and OEGMA were added to water and uniformly dispersed by stirring. Next, KPS and TEMED were added to the solution, then mixture was transferred to a rod-shaped glass vessel (interior size: 5 mm diameter, 300 mm length) and the nanocomposite (NC) hydrogel was obtained after polymerization at room temperature for 24 h. Oxygen was excluded from the system by applying a continuous nitrogen flow. The obtained NC hydrogel was defined as Cm-(M$_{1-x}$O$_x$)*n*, where C, M, and O represented clay, MEO$_2$MA and OEGMA, respectively, and the subscripts *m* and *n* stood for the mass fraction of clay and comonomer, and *x* represented the molar ratio of OEGMA. Meanwhile, organic cross-linked (OR) hydrogel was prepared by the same procedure, except for using NMBA instead of clay.

2.3. Structure characterization

The NC hydrogel samples were frozen in liquid nitrogen and freeze-dried in liophilizer for 48 h to remove the water. Fourier transform infrared (FTIR) spectra of the dried samples were recorded on a Nicolet 6700 spectrometer equipped with attenuated total reflection (ATR) in the region of 4000–600 cm^{-1} at a resolution of 4 cm^{-1}. To evaluate the dispersion of the clay in NC hydrogels, X-ray diffraction (XRD) patterns were performed on a Rigaku D/max 2550 PC diffractometer using Cu Kα (λ = 1.5406 Å) radiation in the 2θ range from 3° to 18° at a voltage of 40 kV and a current of 200 mA. The cross-section images of the freeze-dried hydrogel were captured with a JSM-5600LV scanning electron microscopy (SEM) instrument.

2.4. Swelling/deswelling measurements

As-prepared hydrogels were cut into sections of 50 mm in length, and dried in oven at 40 °C. The dried hydrogels were then immersed in a large excess of water at 25 °C for 400 h to reach swelling equilibrium. Then, the hydrogels in the equilibrium state at 25 °C were transferred to 50 °C water bath to deswell. Three duplicate samples of each NC hydrogel were prepared for swelling/deswelling experiment to guarantee the reproducibility. At the scheduled time, the swollen hydrogels were taken out of the water and weighed after removing the excess water on the surface. The equilibrium swelling ratio (ESR) was calculated by the following equation:

$$\mathrm{ESR} = (W_s - W_d)/W_d \times 100 \quad (1)$$

where W_s and W_d are the weights of swollen hydrogel in equilibrium and the corresponding dried hydrogel, respectively. The water retention (WR) of the hydrogels at 50 °C water bath was determined as follows:

$$\mathrm{WR} = (W_t - W_d)/(W_0 - W_d) \times 100 \quad (2)$$

where W_t is the weight of swollen hydrogel at time *t*, W_0 is the weight of the initial hydrogel at 50 °C, and other symbols represent the meanings defined above. A semilogarithmic plot was introduced to discuss the deswelling kinetics of NC hydrogels with different chemical compositions [41,42]. The time dependence of deswelling kinetics was described as:

$$\ln[(W_t - W_e)/(W_0 - W_e)] = -kt \quad (3)$$

where *k* and *t* represent the rate constant and deswelling time, respectively, W_e is the weight of hydrogel in the deswelling equilibrium state, and other symbols are the same as mentioned above. To investigate the reversible swelling/deswelling behaviors, the swollen hydrogels in equilibrium were alternately moved into water bath at 50 °C and 25 °C and stayed for 48 h to reach new equilibrium after each transition. The time dependence of swelling ratio (SR) was represented by:

$$\mathrm{SR} = (W_t - W_d)/W_d \times 100 \quad (4)$$

where W_t is the weight of swollen hydrogel at time *t*, W_d is the weight of corresponding dried hydrogel. In addition, the equation of temperature-dependent swelling ratio for NC hydrogels was the same as Eq. (4) mentioned above.

3. Results and discussion

Novel thermosensitive NC hydrogels were synthesized by *in-situ* free radical polymerization of MEO$_2$MA and OEGMA using inorganic clay as cross-linker, as shown in Scheme 1. Inhere, the NC hydrogels were physically cross-linked not only due to the chelation by which the polymer chains bind non-covalently to the charged surfaces of the inorganic clay, but also due to the molecular interaction between the ether oxygen of OEGMA and MEO$_2$MA [38]. By combining PEG-derivatives with silicate nanoplatelets, clay/P(MEO$_2$MA-*co*-OEGMA) NC hydrogels featuring homogenous network structure, specific transmittance, and excellent temperature responsiveness were obtained. We investigated the structure of the NC hydrogels and the effects of different chemical compositions on the swelling/deswelling properties. Furthermore, it was found that the volume phase transition temperature (VPTT) of Cm-(M$_{0.8}$O$_{0.2}$)*n* NC hydrogels, of which the molar ratio of MEO$_2$MA and OEGMA was 80 mol%: 20 mol%, was near 40 °C, which is close to human physiological temperature, indicating its potential use as biomaterials.

3.1. Structure of the hydrogels

The investigation of the chemical structure for five representative samples was conducted by ATR-FTIR spectroscopy. As shown in Fig. 1, the asymmetric and symmetric stretching vibrations of CH_2 were determined by the absorption bands at 2931 cm^{-1} and 2882 cm^{-1}, respectively. The absorption bands at 1722, and 1102 cm^{-1} were attributed to the stretching vibrations of C═O, and C—O—C, respectively, in the ester oxygen of oligo(ethylene glycol) based monomers and hydrogels [30]. After polymerization the characteristic absorption of unsaturated C═C double bond at 1635 cm^{-1} disappeared completely. The peak at 1005 cm^{-1} was assigned to the stretching vibration of Si—O in the inorganic clay. Therefore, the characteristic absorption peaks of both OR hydrogel and inorganic clay indicated that NC hydrogel was prepared successfully.

The XRD patterns were carried out using various samples as shown in Fig. 2. A typical diffraction pattern of clay showed a very intensive peak at $2\theta = 7.2°$, which is corresponding to 1.2 nm layer spacing regular stacked clay sheets [43]. And no distinct diffraction peak or crystalline peak was observed in the range from 3° to 18° in the pattern of the dried OR hydrogel. Moreover, the diffraction peak of clay also disappeared in the pattern of the dried NC hydrogel, indicating that the inorganic cross-linker clay has been exfoliated completely and dispersed uniformly in the NC hydrogels.

Fig. 3 shows SEM images of the cross-section of freeze-dried hydrogel samples. The neat and flat structure is observed in OR hydrogel (Fig. 3a), possibly due to the collapse of all pores during the drying process. In contrast, NC hydrogels featured a uniform porous structure after the inorganic clay was introduced in hydrogel network via physical cross-linking, and the nanocomposite structure might result in a mechanical stabilization of the pores during the drying process. The influence of the cross-linking density on the internal morphology of NC hydrogels is shown in Fig. 3b–d. The pore size of NC hydrogels decreased with the increase of clay content, leading to a more homogeneous and compact porous structure with diameters in the range of 5–20 μm. The results implied that higher contents of clay acting as more physical cross-linking junctions increased the cross-linking density in the polymeric network and the porosity. As a consequence, the porous structure of NC hydrogels would facilitate water molecules diffusing in and out compared to OR hydrogel.

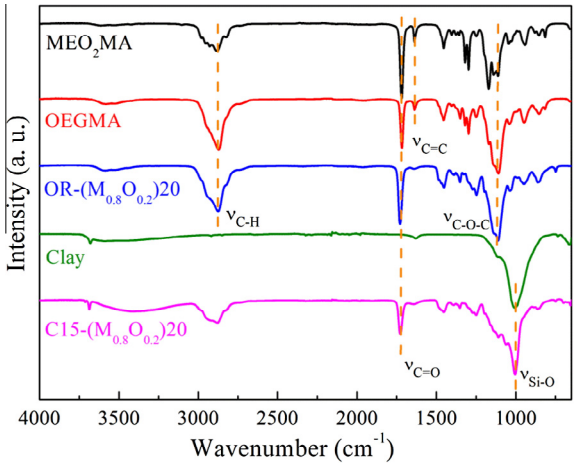

Fig. 1. ATR-FTIR spectra of MEO_2MA monomer, OEGMA monomer, OR-$(M_{0.8}O_{0.2})$20 hydrogel, inorganic clay, and C15-$(M_{0.8}O_{0.2})$20 NC hydrogel.

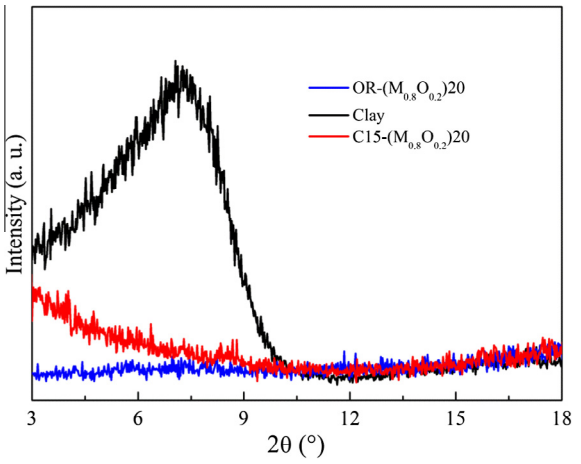

Fig. 2. The XRD patterns of OR-$(M_{0.8}O_{0.2})$20 hydrogel, inorganic clay, and C15-$(M_{0.8}O_{0.2})$20 NC hydrogel. All samples were milled powders after freeze-drying.

3.2. Swelling behavior of P(MEO_2MA-co-OEGMA) NC hydrogels

The influence of the compositions on the swelling behavior of thermosensitive clay/P(MEO_2MA-*co*-OEGMA) NC hydrogels in water at 25 °C is shown in Fig. 4. Generally, physically cross-linked NC hydrogels rapidly attained the maximum swelling ratio and then began to deswell until the equilibrium state is reached, while the swelling ratio of chemically cross-linked OR hydrogel (Fig. S1) increased with time and directly reached a constant value without deswelling process. The characteristic swelling/deswelling mechanism of clay/P(MEO_2MA-*co*-OEGMA) NC hydrogels might be attributed to the synergetic effects of the clay/polymer hydrogels as polyelectrolyte hydrogels, and the continuous release of ions from the network in the course of swelling process [17,44,45]. Thus, the osmotic swelling pressure of ions inside the hydrogel decreased, leading to the deswelling of the hydrogels.

On the other hand, a series of C5-$(M_{1-x}O_x)$20 NC hydrogels were synthesized with 5 wt% clay as cross-linker by employing a different amount of OEGMA. The swelling properties of these C5-$(M_{1-x}O_x)$20 NC hydrogels at 25 °C are shown in Fig. 4a and b. The equilibrium degree of swelling increased from 850% to 2308% when the molar ratio of hydrophilic OEGMA units increased from 0 mol% to 100 mol%. It indicated that the equilibrium swelling ratio of the NC hydrogels increased when increasing the

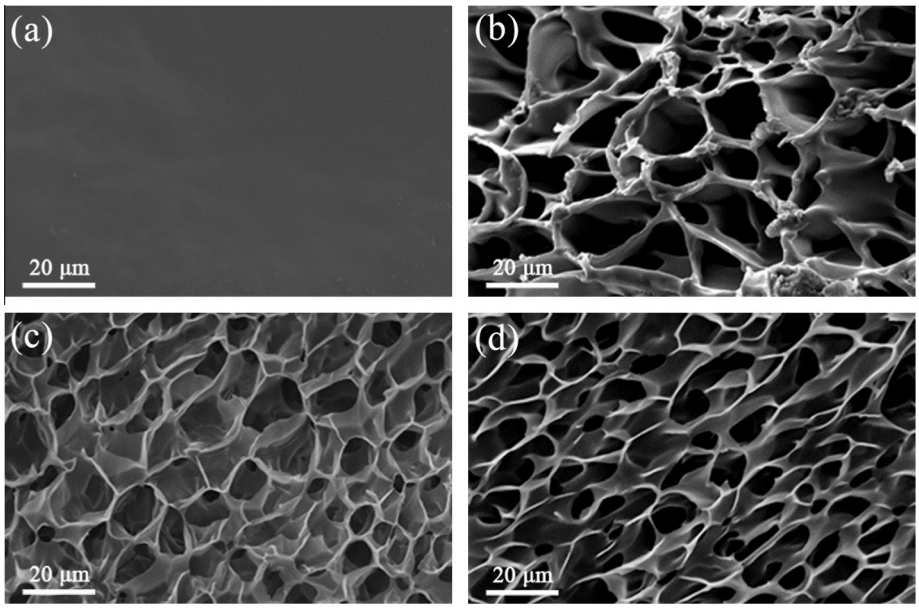

Fig. 3. SEM images of (a) OR-($M_{0.8}O_{0.2}$)20, (b) C5-($M_{0.8}O_{0.2}$)20, (c) C10-($M_{0.8}O_{0.2}$)20, and (d) C15-($M_{0.8}O_{0.2}$)20 freeze-dried hydrogels.

hydrophilic ethylene glycol side chains of OEGMA, which improved the water absorbing capacity of NC hydrogels. Besides the influence of balance between hydrophilicity and hydrophobicity of copolymer units, the equilibrium degree of swelling was also affected by the cross-linking density of network. Cm-($M_{0.8}O_{0.2}$)20 hydrogels with various contents of inorganic clay as physical cross-linkers were fabricated to discuss their swelling behavior (Fig. 4c and d). It was observed that the swelling ratio of the hydrogels decreased with the increase of density of physical cross-linking points. And the Cm-($M_{0.8}O_{0.2}$)20 NC hydrogels with higher cross-linking density exhibited a significant decline in equilibrium swelling ratio. In addition, with the increase of polymer concentration, the equilibrium swelling ratio of the C5-($M_{0.8}O_{0.2}$)*n* NC hydrogels decreased rapidly (Fig. 4e and f). This might be attributed to that, at higher concentration of the polymer matrix, the stronger molecular interaction between OEGMA and MEO_2MA increased the number of cross-linking points in the hydrogels, leading to the decrease of the equilibrium swelling ratio consequently [38]. All in all, the maximum degree of swelling for clay/P(MEO_2MA-*co*-OEGMA) NC hydrogels was more than 2500%, which was six times higher than that of P(MEO_2MA-*co*-OEGMA) hydrogels cross-linked by triethylene glycol dimethacrylate (TEGDMA) [36].

3.3. Deswelling kinetics of hydrogels in response to temperature change

The investigation of deswelling kinetics is important for smart hydrogels in measuring their water retention and deswelling rate. Fig. 5 shows the deswelling kinetics of clay/P(MEO_2MA-*co*-OEGMA) NC hydrogels from the equilibrium swelling state at 25 °C water bath to 50 °C water bath. As expected, all the swollen hydrogels tended to shrink and lose water after immersing in water at higher temperature due to the disruption of hydrophilic/hydrophobic balance in NC hydrogels. The trends of deswelling curves of clay/P(MEO_2MA-*co*-OEGMA) NC hydrogels are similar with those of OR hydrogel (Fig. S2) and traditional hydrogels based on PNIPAM [16], that is, the water retention decreased rapidly with the increase of deswelling time before reaching a constant value within 24 h. For the series of C5-($M_{1-x}O_x$)20 NC hydrogels, it was found that the higher the ratio of MEO_2MA was, the quicker the deswelling behavior performed (Fig. 5a). Here, with the increase of MEO_2MA units, the water retention decreased from 70% for C5-(M_0O_1)20 hydrogel to 13% for C5-(M_1O_0)20 hydrogel after immersing in 25 °C water for 6 h, indicating that the molar ratio significantly affected the water retention. The lower water retention of C5-($M_{1-x}O_x$)20 hydrogels could be ascribed to the presence of more hydrophobic short ethylene glycol side chains in the NC hydrogels, and the short ethylene glycol side chains would potentially act as water-release channels in the network and facilitate the deswelling process. Similarly, the effect of cross-linking density on the deswelling behavior of NC hydrogels is shown in Fig. 5b. Here, the water retention increased rapidly with the decrease of clay content. The shrinkage of NC hydrogels was almost complete within 12 h, even though the water temperature (50 °C) was only slightly higher than their VPTT about 40 °C. Especially, when the clay content was higher than 10 wt%, the deswelling ratio of Cm-($M_{0.8}O_{0.2}$)20 hydrogels was also decreased. This is not in accordance with clay/PNIPAM hydrogels [16,17], of which the strong amide-amide hydrogen bonding and high cross-linking density restricted the shrinkage of NC hydrogels. As shown in Fig. 5c, C5-($M_{0.8}O_{0.2}$)10 NC hydrogels containing the lowest concentration of polymer

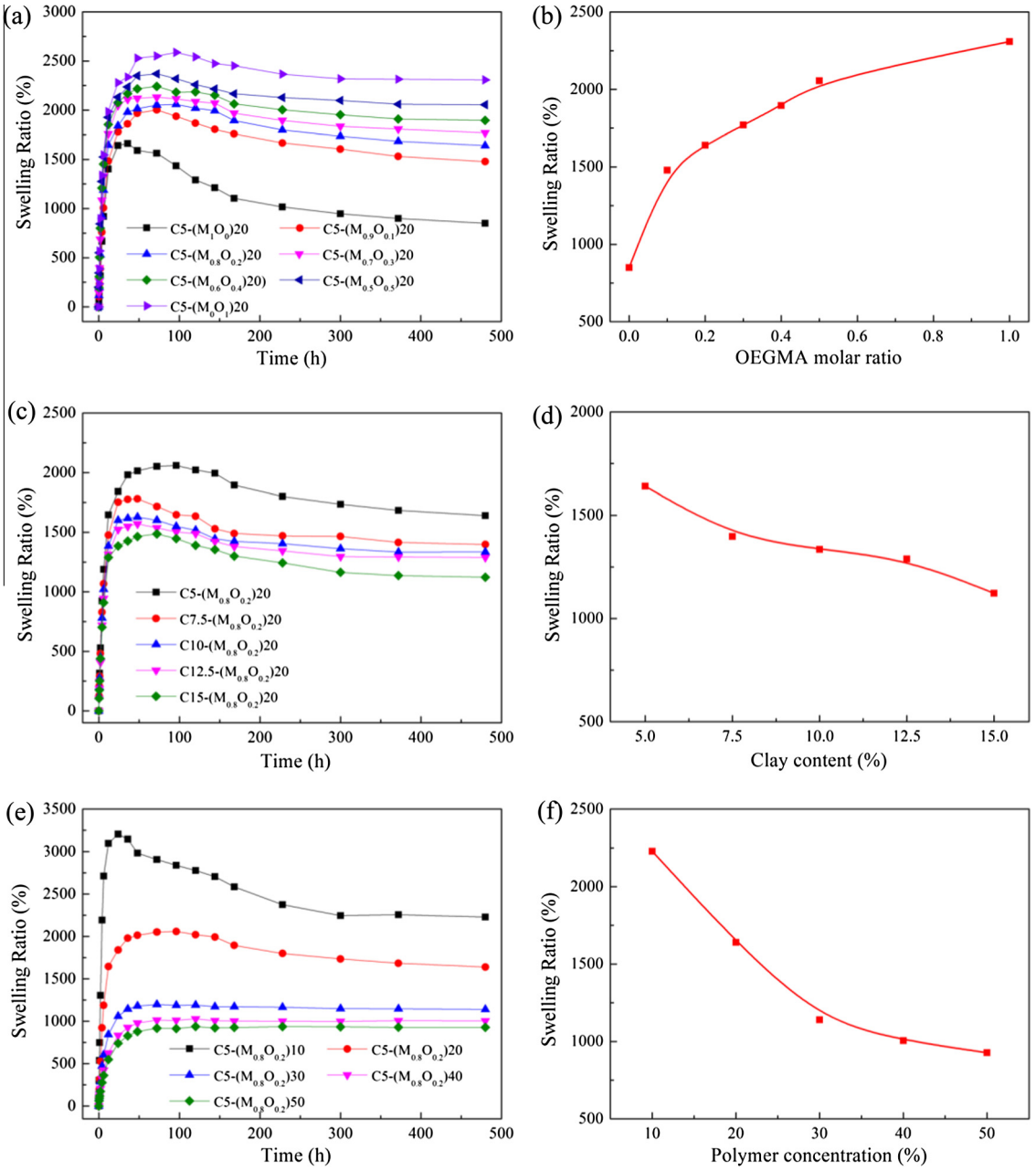

Fig. 4. Swelling ratios of NC hydrogels in water as a function of swelling time. Effect of the (a, b) comonomer molar ratio, (c, d) clay content, and (e, f) polymer concentration on swelling behavior of clay/P(MEO_2MA-*co*-OEGMA) NC hydrogels at 25 °C.

matrix exhibited the highest water retention. However, when the polymer concentration was higher than 10 wt%, the water retention of all these samples was prone to decrease to a common value of 20%. This is possibly because considerable amount of ethylene glycol units in C5-($M_{0.8}O_{0.2}$)50 NC hydrogels facilitated stronger hydrogen bond interaction between the copolymer, seriously limiting the transition of polymer chains from hydrophilic state to a hydrophobic state.

As shown in Fig. 5d–f, the linear fit curves of $\ln[(W_t - W_e)/(W_0 - W_e)]$ versus time for the deswelling of NC hydrogels had a correlation coefficient (R^2) of more than 0.95, and can be used to well reflect the deswelling kinetics of clay/P(MEO_2MA-*co*-OEGMA) NC hydrogels. Hence, the first-order kinetic constant (k) calculated from the linear fitting of the experimental results to Eq. (3) was chosen to conduct the quantitative study and compare the deswelling rates of swollen hydrogels with different chemical compositions. Equilibrium swelling/deswelling ratio, k, and R^2 for clay/P(MEO_2MA-*co*-OEGMA) NC hydrogels with different chemical compositions are listed in Table 1. The k value of the C5-($M_{1-x}O_x$)20 NC hydrogels with a higher MEO_2MA content was higher than that of the hydrogel with a higher amount of OEGMA (Fig. 5d),

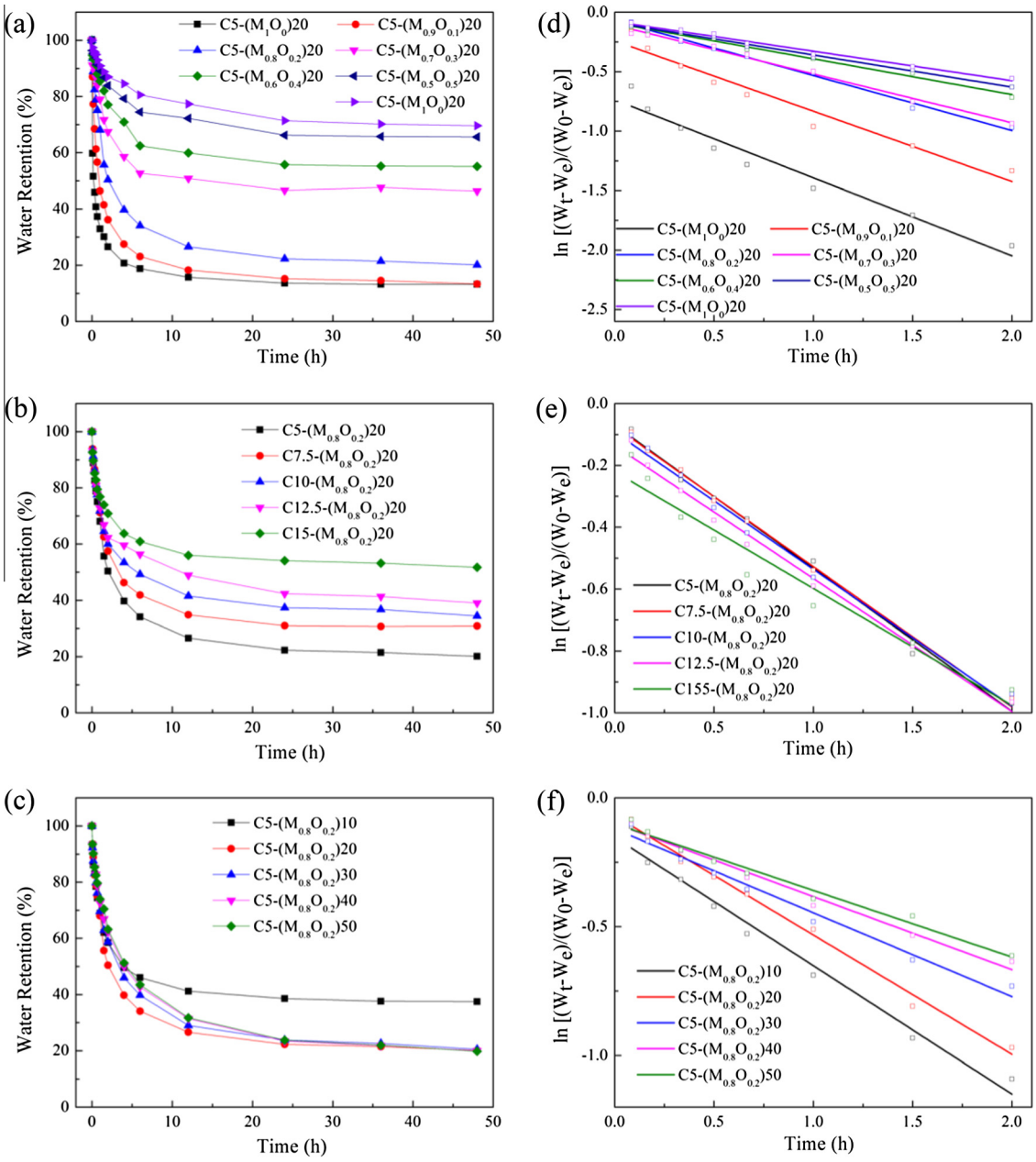

Fig. 5. Deswelling kinetics for NC hydrogels with series of (a) comonomer molar ratio, (b) clay content, and (c) polymer concentration at 50 °C. The linear fit curves of $\ln[(W_t - W_e)/(W_0 - W_e)]$ versus time for the deswelling rates of NC hydrogels (d–f) at 50 °C.

indicating that higher content of MEO_2MA in hydrogels contributed to a higher deswelling rate. The reasons might be that hydrophobic short ethylene glycol side chains in the NC hydrogels would act as water-release channels to further facilitate the deswelling process. As shown in Fig. 5e, the deswelling rate of C5-($M_{0.8}O_{0.2}$)20 hydrogel was higher than that of C15-($M_{0.8}O_{0.2}$)20 hydrogel, and the k value gradually increased with the decreasing of the amount of physical cross-linker, which meant that the deswelling rate decreased. Furthermore, the effect of polymer concentration on the deswelling kinetics of C5-($M_{0.8}O_{0.2}$)n NC hydrogels is given in Fig. 5f. The NC hydrogels with less polymer concentration had a higher deswelling rate than those of NC hydrogels with higher polymer concentration. It would be mainly attributed to the enhanced intermolecular interaction among ethylene glycol side chains in NC hydrogels with higher polymer concentration.

3.4. Reversible stimulus response of clay/P(MEO_2MA-co-OEGMA) NC hydrogels

As discussed above, the NC hydrogels possessed a controllable swelling and deswelling behavior in water. Considering the potential applications in biomedical

Table 1
Equilibrium swelling ratio (ESR), deswelling ratio (DSR), water retention (WR), first-order kinetic constant (k), and the correlation coefficient (R^2) of clay/P(MEO_2MA-*co*-OEGMA) NC hydrogels with different compositions.

Samples	25 °C ESR (%)	50 °C DSR (%)	50 °C WR (%)	k	R^2
C5-(M_1O_0)20	850	112	13	0.6554	0.9488
C5-($M_{0.9}O_{0.1}$)20	1478	197	13	0.5914	0.9507
C5-($M_{0.8}O_{0.2}$)20	1640	329	20	0.4627	0.9926
C5-($M_{0.7}O_{0.3}$)20	1769	820	46	0.4112	0.9907
C5-($M_{0.6}O_{0.4}$)20	1895	1045	55	0.3010	0.9883
C5-($M_{0.5}O_{0.5}$)20	2056	1348	65	0.2704	0.9913
C5-(M_0O_1)20	2308	1606	69	0.2481	0.9863
C7.5-($M_{0.8}O_{0.2}$)20	1397	431	31	0.4533	0.9961
C10-($M_{0.8}O_{0.2}$)20	1335	459	34	0.4427	0.9901
C12.5-($M_{0.8}O_{0.2}$)20	1288	503	39	0.4298	0.9879
C15-($M_{0.8}O_{0.2}$)20	1123	581	51	0.3776	0.9440
C5-($M_{0.8}O_{0.2}$)10	2228	835	37	0.4982	0.9782
C5-($M_{0.8}O_{0.2}$)30	1140	233	20	0.3254	0.9801
C5-($M_{0.8}O_{0.2}$)40	1005	201	20	0.2838	0.9812
C5-($M_{0.8}O_{0.2}$)50	927	183	19	0.2588	0.9761

materials, it is necessary to evaluate their reversible stimulus response. Fig. 6 shows the time dependence of the oscillatory swelling/deswelling behavior of NC hydrogels with different chemical compositions. Compared to OR hydrogel (Fig. S3), NC hydrogels exhibited a remarkable and reversible swelling and deswelling change in response to the alternating temperatures of 50 °C and 25 °C. As shown in Fig. 6a, almost all C5-($M_{1-x}O_x$)20 NC hydrogels could keep their initial equilibrium swelling ratio except C5-(M_1O_0)20 hydrogel due to its VPTT (around 10 °C) was much lower than the environmental temperature. With the increase of the MEO_2MA molar ratio, the reversible swelling ratio of C5-($M_{1-x}O_x$)20 NC hydrogels gradually decreased. Moreover, in Fig. 6b, Cm-($M_{0.8}O_{0.2}$)20 NC hydrogels with different cross-linking densities exhibited a reversible swelling/deswelling transformation behavior because their VPTT (around 40 °C) was between the alternating temperatures, and Cm-($M_{0.8}O_{0.2}$)20 NC hydrogels with lower clay content exhibited higher swelling ratio at 25 °C and lower swelling ratio at 50 °C. Thus, the swelling ratios of Cm-($M_{0.8}O_{0.2}$)20 NC hydrogels with lower cross-linking densities varied more significantly than those of NC hydrogels with higher cross-linking densities, and this implied that the incorporation of clay made the hydrogels more sensitive to temperature, resulting in a larger thermosensitive volume change. This reversible characteristics was quite different from those of C5-($M_{1-x}O_x$)20 NC hydrogels mentioned above and the result was possibly attributed to the high cross-linking density in NC hydrogel networks, which restricted the copolymer chains movement. Furthermore, the swelling/deswelling curves of C5-($M_{0.8}O_{0.2}$)n NC hydrogels with different polymer concentration showed a similar trend with the curves of C5-($M_{1-x}O_x$)20 NC hydrogels (Fig. 6c). The samples with higher polymer concentration had a lower value of swelling ratio, due to the strong hydrogen bond interaction of ethylene glycol side chains in polymer matrix. The reversible thermosensitivity was demonstrated by the fact that the clay/P(MEO_2MA-*co*-OEGMA) hydrogels had excellent sensitivity to temperatures alternating between 50 °C and 25 °C. The thermosensitive swelling/deswelling changes could be controlled within a large range by varying molar ratio, clay content, and polymer concentration. Thus, a hydrogel with a desirable swelling ratio would be obtained by controlling the chemical composition.

3.5. Temperature dependent properties of NC hydrogels

According to the work mentioned above, clay/P(MEO_2MA-*co*-OEGMA) NC hydrogels featured a temperature-dependent responsiveness, and exhibited remarkable deswelling behaviors in response to external temperature (Fig. 7). The digital photos of three hydrogel samples with 20 mol%, 40 mol%, and 100 mol% of OEGMA clearly show their temperature responsiveness (Fig. 7a). It was observed that the shape and transmittance of NC hydrogels seemed to be dependent on the environmental temperature, and the diameter and length of these NC hydrogels both shrunk as temperature increased. Each sample was transparent and swollen at an initial temperature of 25 °C. When the temperature increased to 50 °C, i.e. above the VPTT of C5-($M_{0.8}O_{0.2}$)20, it immediately became opaque and shrank. The other two samples, of which the VPTTs were over 50 °C, were still transparent at 50 °C. This change of transmittance might be attributed to the disruption of the hydrophilic/hydrophobic balance when temperature alters in C5-($M_{0.8}O_{0.2}$)20 hydrogel, that is, hydrogels were completely transparent at low temperatures (T < VPTT), but became opaque at higher temperatures (T > VPTT).

Fig. 7b shows the temperature dependence of NC hydrogels with various OEGMA contents on the swelling ratio. It took about 48 h for NC hydrogels to release water and then a new swelling equilibrium was achieved under the specific temperature condition. The equilibrium swelling ratio of all the samples decreased as the temperature gradually increased. What's more, the change of sample from one equilibrium swelling state to another is not instantaneous, so that the process is in agreement with OR hydrogel (Fig. S4), but not in accordance with PNIPAM based hydrogels [3,46], indicating that the P(MEO_2MA-*co*-OEGMA) based hydrogels were suitable for slow-releasing applications. It was also observed that the

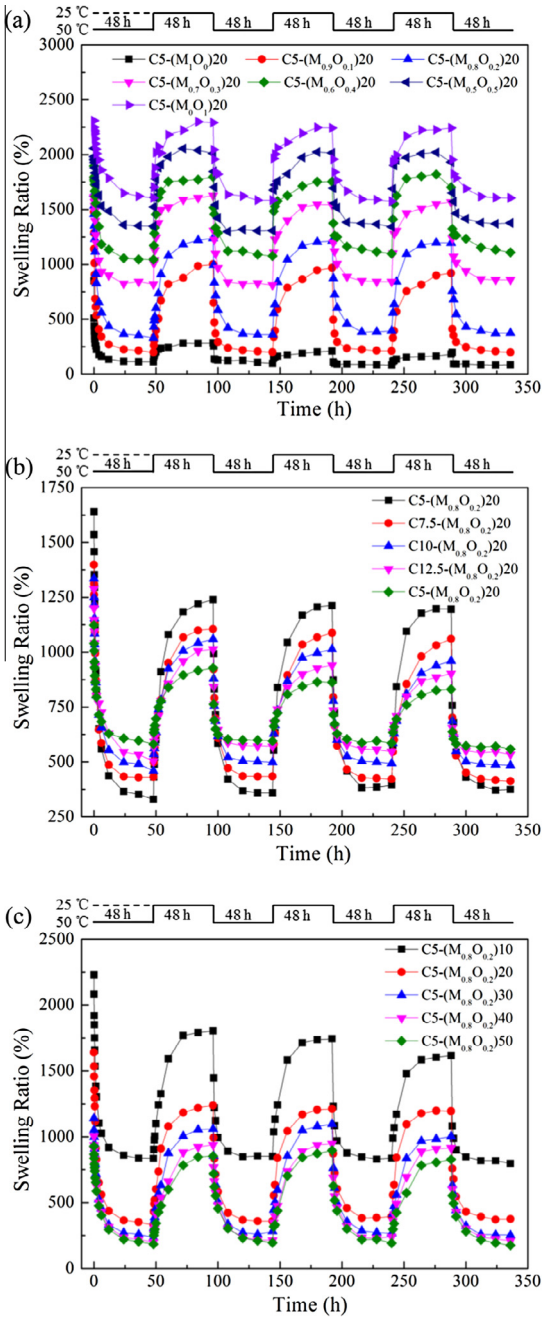

Fig. 6. Oscillatory swelling behavior of NC hydrogel upon temperature changes between 50 °C and 25 °C. The swelling and deswelling ratio changes with different (a) comonomer molar ratio, (b) clay content, (c) polymer concentration, respectively.

higher hydrophobic character of the MEO_2MA, compared to OEGMA, led to a slight decrease of the swelling ratio of the NC hydrogels. Fig. 7c shows the temperature dependence of the swelling behavior of Cm-($M_{0.8}O_{0.2}$)20 NC hydrogels with different mass fraction of clay. It should be noted that the relationship between swelling ratio and clay content for Cm-($M_{0.8}O_{0.2}$)20 NC hydrogels at lower temperature (T < VPTT) was quite different from that of hydrogels at higher temperature (T > VPTT). For example, the swelling ratio of Cm-($M_{0.8}O_{0.2}$)20 hydrogel decreased from 1905% to 1330% with the increase of clay content from 5 wt% to 15 wt% at 5 °C. However, the swelling ratio of the hydrogels increased from 32% to 282% along with the same clay content at 90 °C. This characteristic can be attributed to the high cross-linking density in the networks, which suppressed the change of thermosensitive copolymer chains from a hydrophilic state to a hydrophobic state when the temperature was above the VPTT. Particularly, the swelling ratio decreased remarkably when the clay content was higher than 10 wt%, which was different from that of clay/PNIPAM hydrogels [16,17]. The volume of clay/PNIPAM hydrogels was hard to shrink due to the amide-amide hydrogen bonding among PNIPAM polymer chains that were much stronger than the molecular interaction among ethylene glycol side chains in the polymer matrix for the same cross-linking density. In order to compare the thermosensitivity of NC hydrogels with different polymer concentration, the swelling ratios of C5-($M_{0.8}O_{0.2}$)n hydrogels at a series of temperatures were presented in Fig. 7d. With the increase of the temperature, the equilibrium swelling ratio decreased to 30%. Generally speaking, the desired swelling ratio for this kind of NC hydrogels can be tailored by controlling both the chemical composition and external temperature. Owing to the biocompatibility of oligo(ethylene glycol) methacrylate based polymers and the wide thermosensitive range demonstrated in this study, these novel clay/P(MEO_2MA-*co*-OEGMA) NC hydrogels could replace PNIPAM based hydrogels as biomaterials.

4. Conclusions

In this study, clay/P(MEO_2MA-*co*-OEGMA) hydrogels based on two kinds of non-linear PEG derivatives, MEO_2MA and OEGMA, were synthesized in the presence of physical clay as cross-linker via *in-situ* free radical polymerization. The incorporation of exfoliated clay in the NC hydrogels had significant influence on the microstructure and swelling/deswelling behaviors of P(MEO_2MA-*co*-OEGMA) based hydrogels. The NC hydrogels featured a homogeneous porous structure, which could facilitate water to diffuse in and out of the networks. Besides, the swelling/deswelling kinetics of a series of NC hydrogels with various chemical compositions was systematically investigated under different environmental temperatures. We could prove that the equilibrium swelling ratio and water retention of NC hydrogels increased with increasing the fraction of hydrophilic OEGMA, but with decreasing of the polymer concentration. However, as the inorganic cross-linker content increased, the equilibrium swelling ratio of NC hydrogels improved while the water retention reduced. The deswelling rates of NC hydrogels were in accordance with the first-order kinetics, indicating that a higher deswelling rate could be reached by reducing the fraction of OEGMA, clay, and polymer, respectively. In addition, higher temperature led to the change of hydrophilic/hydrophobic balance of thermosensitive NC hydrogels. Therefore, according to these unique and significant results, the physical properties of

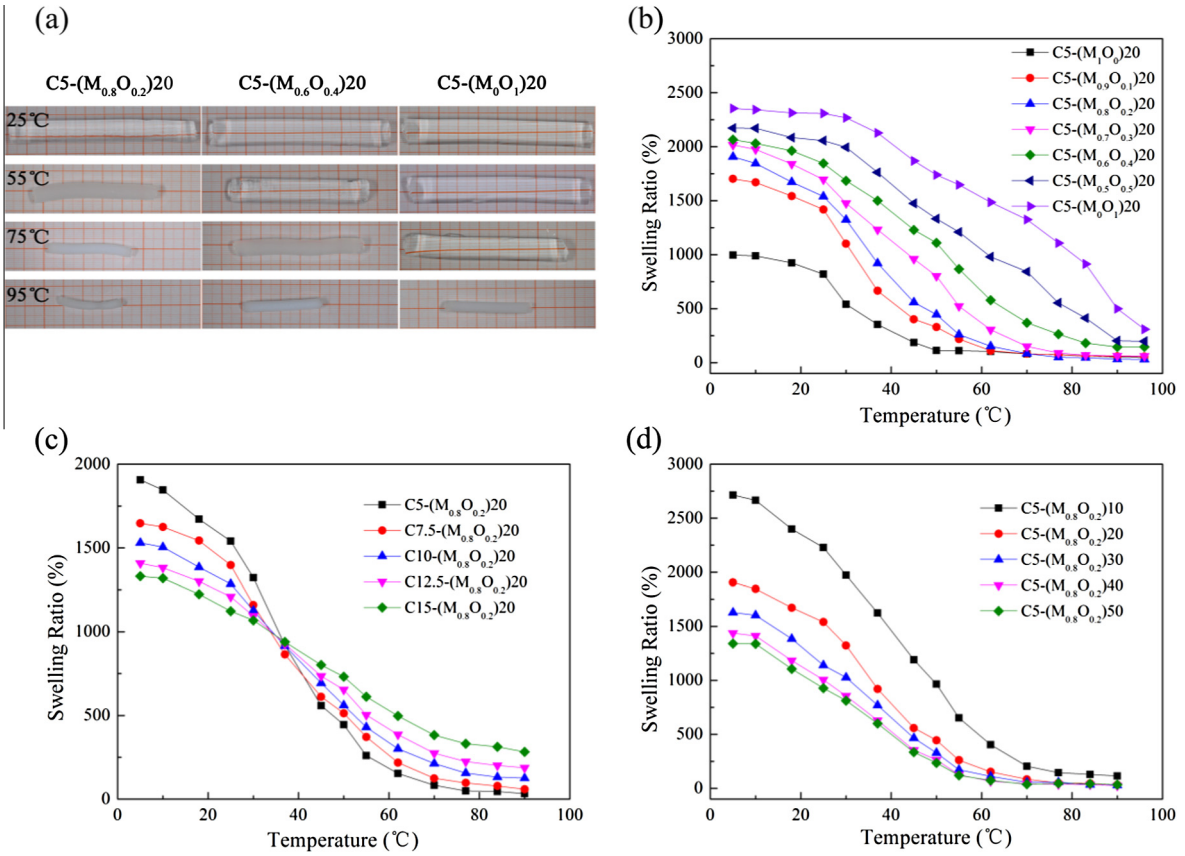

Fig. 7. (a) Photographs of the NC hydrogels with various OEGMA at different temperature. Temperature dependence of the swelling behavior of clay/P(MEO_2MA-*co*-OEGMA) NC hydrogels with different compositions: (b) comonomer molar ratio, (c) clay content, (d) polymer concentration, respectively.

clay/P(MEO_2MA-*co*-OEGMA) NC hydrogels, such as equilibrium swelling/deswelling ratio, water retention, reversible response, and temperature dependence behaviors, could be effectively controlled by the internal chemical composition and external temperature. And these novel NC hydrogels with tunable swelling/deswelling characteristics, distinct thermosensitivity, as well as the excellent biocompatibility are promising candidates for applications in drug delivery, tissue engineering, biosensors, optics, etc.

Acknowledgements

This work was financially supported by Program for Changjiang Scholars and Innovative Research Team in University (T2011079, IRT1221), National High-Tech Research and Development Program of China (2012AA030309), Chinese Universities Scientific Fund (CUSF-DH-D-2014022), as well as National Natural Science Foundation for Distinguished Young Scholar of China (50925312).

Appendix A. Supplementary material

Supplementary data associated with this article can be found, in the online version, at http://dx.doi.org/10.1016/j.eurpolymj.2015.03.072.

References

[1] Seliktar D. Science 2012;336(6085):1124.
[2] Annabi N, Tamayol A, Uquillas JA, Akbari M, Bertassoni LE, Cha C, Camci-Unal G, Dokmeci MR, Peppas NA, Khademhosseini A. Adv Mater 2014;26(1):85.
[3] Xia L, Xie R, Ju X, Wang W, Chen Q, Chu L. Nat Commun 2013;4:2226.
[4] Lu Y, Ballauff M. Prog Polym Sci 2011;36(6):767.
[5] Cheng Y, Xia M, Meng Z, Wu Y, Ren H, Jiang Y, Liu Y, Zhou Z, Jiang X, Zhu M. Acta Polym Sin 2014;10:1342.
[6] Zhang Y, Yang B, Zhang X, Xu L, Tao L, Li S, Wei Y. Chem Commun 2012;48(74):9305.
[7] Xia M, Wang Y, Zhang Y, Cheng Y, Chen S, Wang R, Meng Z, Zhu M. Aust J Chem 2014;67(1):112.
[8] Wang Z, Xu X, Chen C, Yun L, Song J, Zhang X, Zhuo R. ACS Appl Mater Interfaces 2010;2(4):1009.
[9] Yang B, Zhang Y, Zhang X, Tao L, Li S, Wei Y. Polym Chem 2012;3(12):3235.
[10] Zhang Y, Tao L, Li S, Wei Y. Biomacromolecules 2011;12(8):2894.
[11] Hirokawa Y, Tanaka T. J Chem Phys 1984;81(12):6379.
[12] Alarcon CdlH, Pennadam S, Alexander C. Chem Soc Rev 2005;34(3):276.
[13] Satarkar N, Hilt J. J Control Release 2008;130(3):246.
[14] Ma X, Li Y, Wang W, Ji Q, Xia Y. Eur Polym J 2013;49(2):389.
[15] Haraguchi K, Takehisa T. Adv Mater 2002;14(16):1120.
[16] Haraguchi K, Takehisa T, Fan S. Macromolecules 2002;35(27):10162.
[17] Liu Y, Zhu M, Liu X, Zhang W, Sun B, Chen Y, Adler HJP. Polymer 2006;47(1):1.
[18] Wang T, Zheng S, Sun W, Liu X, Fu S, Tong Z. Soft Matter 2014;10(19):3506.
[19] Zhu M, Liu Y, Sun B, Zhang W, Liu X, Yu H, Zhang Y, Kuckling D, Adler HJP. Macromol Rapid Commun 2006;27(13):1023.
[20] Roy D, Cambre JN, Sumerlin BS. Prog Polym Sci 2010;35(1–2):278.

[21] Wang Q, Mynar J, Yoshida M, Lee E, Lee M, Okuro K, Kinbara K, Aida T. Nature 2010;463(7279):339.
[22] Gaharwar AK, Schexnailder PJ, Kline BP, Schmidt G. Acta Biomater 2011;7(2):568.
[23] Ozcelik B, Blencowe A, Palmer J, Ladewig K, Stevens GW, Abberton KM, Morrison WA, Qiao GG. Acta Biomater 2014;10(6):2769.
[24] Vancoillie G, Frank D, Hoogenboom R. Prog Polym Sci 2014;39(6):1074.
[25] Roth PJ, Jochum FD, Theato P. Soft Matter 2011;7(6):2484.
[26] Tang L, Yang Y, Bai T, Liu W. Biomaterials 2011;32(7):1943.
[27] Lutz J-F, Akdemir Ö, Hoth A. J Am Chem Soc 2006;128(40):13046.
[28] Lutz J-F, Hoth A. Macromolecules 2006;39(2):893.
[29] Lutz J-F. J Polym Sci Part A: Polym Chem 2008;46(11):3459.
[30] Sun S, Wu P. Macromolecules 2012;46(1):236.
[31] Yao Z, Tam KC. Polymer 2012;53(16):3446.
[32] Peng B, Grishkewich N, Yao Z, Han X, Liu H, Tam KC. ACS Macro Lett 2012;1(5):632.
[33] Xia M, Cheng Y, Meng Z, Jiang X, Chen Z, Theato P, Zhu M. Macromol Rapid Commun 2015;36(5):477.
[34] Cai T, Marquez M, Hu Z. Langmuir 2007;23(17):8663.
[35] Chi C, Cai T, Hu Z. Langmuir 2009;25(6):3814.
[36] París R, Quijada-Garrido I. Eur Polym J 2009;45(12):3418.
[37] París R, Quijada-Garrido I. Eur Polym J 2010;46(11):2156.
[38] Wang Y, Chen D. J Colloid Interface Sci 2012;372(1):245.
[39] Smeets NMB, Bakaic E, Patenaude M, Hoare T. Chem Commun 2014;50(25):3306.
[40] Hu Z, Cai T, Chi C. Soft Matter 2010;6(10):2115.
[41] Serizawa T, Wakita K, Akashi M. Macromolecules 2002;35(1):10.
[42] Wang Y, Yuan Z, Chen D. J Mater Sci 2012;47(3):1280.
[43] Haraguchi K, Li H, Matsuda K, Takehisa T, Elliott E. Macromolecules 2005;38(8):3482.
[44] Ren H, Zhu M, Haraguchi K. J Colloid Interface Sci 2012;375(1):134.
[45] Ren H, Zhu M, Haraguchi K. Macromolecules 2011;44(21):8516.
[46] Zhang J, Jandt KD. Macromol Rapid Commun 2008;29(7):593.